Elastic Scattering of Negative Pions by Protons at 152 and 226 MeV*

S. KELLMAN,†‡ W. P. KOVACIK,†§ AND T. A. ROMANOWSKI||
Carnegie Institute of Technology, Pittsburgh, Pennsylvania
(Received 13 April 1962)

The differential elastic and total cross sections for the scattering of 152- and 226-MeV negative pions by protons have been measured with a liquid hydrogen target and scintillation counters. Analyses of the incident pion beams with a Čerenkov counter yielded higher electron contents than those deduced from range curves. Elastically scattered pions were distinguished from electrons among the scattered particles by use of a Čerenkov counter, or by demanding a coincidence between the scattered pion and recoil proton. The total cross sections measured were 63.7 ± 2.0 and 52.9 ± 1.4 mb at 152 and 226 MeV, respectively. With the present uncertainties, the real parts of the forward scattering amplitudes agree with the predictions of pion dispersion relations.

I. INTRODUCTION

IN recent years, much work has been done on pion-proton scattering to afford comparison with the theoretical dispersion relations,[1,2] relating the real part of the forward scattering amplitude D to an integral over energy involving the total cross sections. In π^+-p scattering at energies from zero to 400 MeV, good agreement between experimental and theoretical results for D_+ is obtained if a coupling constant of $f^2=0.09\pm0.01$ is used in the dispersion relations. In regard to π^--p scattering, however, Puppi and Stanghellini[3] found that a lower value of f^2 was necessary to obtain agreement between experiment and theory. Since the π^+ and π^- data should be fitted using the same value of f^2, Schnitzer and Salzman,[4,5] using more recent data and performing a more detailed error analysis, re-analyzed the π^-p scattering data. They found much less disagreement than Puppi and Stanghellini, but there existed a residual discrepancy of the same general character which was largest for the 150-, 170-, and 220-MeV measurements of Ashkin *et al.*[6,7] In agreement with other recent studies,[8–10] they found that the theoretical values of D_- have a strong dependence on the detailed shape of the total cross section near resonance. It was suggested, therefore, that further experiments be performed to determine more accurate values of the total cross section and of the real part of the forward scattering amplitude in the energy region from 100 to 300 MeV.

Accordingly, measurements of negative pion scattering by protons were undertaken at 98 MeV at Liverpool,[11] and 130 and 152 MeV at Chicago.[12,13] These experiments revealed an appreciable electron contamination in the scattered pion beam. The Chicago experiment at 152 MeV resulted in a larger value of the total cross section than had been previously measured. Noyes and Edwards,[14] by abandoning the 150 and 170 MeV Carnegie Tech data in favor of the more recent Chicago results, achieved agreement between dispersion theory using $f^2=0.086$ and experimental data up to 220 MeV. At 225 MeV, Deahl[15] reported a total π^- elastic cross section which was 15% lower than that found in the earlier measurement.[7] He obtained a value of D_- that agreed with the curve of Schnitzer and Salzman for $f^2=0.08$, but with a large uncertainty.

In the present measurements at 152 and 226 MeV, as in the Liverpool and Chicago experiments, the scattered pion beam was found to be contaminated with electrons. These electrons were presumably due to charge-exchange scattering in the hydrogen and the conversion of the resulting γ rays in the hydrogen and target walls. Two methods were used to distinguish these electrons from the scattered pions. For those angles at which the recoil proton had sufficient energy to emerge from the liquid hydrogen target, the scattered pion was detected in coincidence with the recoil proton. For the remaining angles, pulse-height analysis of the radiation produced by the scattered particles in a Čerenkov counter was utilized.

One of the largest uncertainties in these cross-section measurements is the composition of the incident pion beam. The present measurements made use of a

* Research partially supported by the U. S. Atomic Energy Commission.

† Theses based upon this work have been submitted by S. Kellman and W. P. Kovacik in partial fulfillment of the requirements for the degree of Doctor of Philosophy at Carnegie Institute of Technology.

‡ Present address: Lawrence Radiation Laboratory, Livermore, California.

§ Present address: Westinghouse Electric Corporation, Atomic Power Department, P. O. Box 355, Pittsburgh 30, Pennsylvania.

|| Present address: Argonne National Laboratory, P. O. Box 299, Argonne, Illinois.

[1] M. L. Goldberger, Phys. Rev. **99**, 979 (1955).
[2] M. L. Goldberger, H. Miyazawa, and R. Oehme, Phys. Rev. **99**, 986 (1955).
[3] G. Puppi and A. Stanghellini, Nuovo Cimento **5**, 1305 (1957).
[4] H. J. Schnitzer and G. Salzman, Phys. Rev. **112**, 1802 (1958).
[5] H. J. Schnitzer and G. Salzman, Phys. Rev. **113**, 1153 (1959).
[6] J. Ashkin, J. P. Blaser, F. Feiner, and M. O. Stern, Phys. Rev. **101**, 1149 (1956).
[7] J. Ashkin, J. P. Blaser, F. Feiner, and M. O. Stern, Phys. Rev. **105**, 724 (1957).
[8] M. H. Zaidi and E. L. Lomon, Phys. Rev. **108**, 1352 (1957).
[9] J. Hamilton, Phys. Rev. **110**, 1134 (1957).
[10] Hong-Yee Chiu, Phys. Rev. **110**, 1140 (1957).
[11] D. N. Edwards, S. G. F. Frank, and J. R. Holt, Proc. Phys. Soc. (London) **73**, 856 (1959).
[12] W. J. Kernan, Phys. Rev. **119**, 1092 (1960).
[13] U. E. Kruse and R. C. Arnold, Phys. Rev. **116**, 1008 (1959).
[14] H. P. Noyes and D. N. Edwards, Phys. Rev. **118**, 1409 (1960).
[15] J. Deahl, M. Derrick, J. Fetkovich, T. Fields, and G. B. Yodh, Phys. Rev. **124**, 1987 (1961).

Čerenkov counter to determine the number of pions in the incident beam.

II. EXPERIMENTAL ARRANGEMENT AND PROCEDURE

A. Pion Beams

Negative pions were produced internally by the circulating 440-MeV protons of the Carnegie Tech synchrocyclotron striking a beryllium target with dimensions of $\frac{1}{2}\times\frac{1}{2}\times1\frac{1}{2}$ in. Two quadrupole magnets mounted on the coil can of the cyclotron served to collect pions diverging vertically from the target, and thereby increased the intensity of the external pion beam by a factor of two. After traversing a channel in twelve feet of shielding wall, pions of the desired momenta were obtained with a selecting magnet. At 226 and 152 MeV, respectively, the monitored incident beam intensity ranged from 1900 to 3500 particles per second. The energies of the pions, as determined from integral range curves taken in copper, were 152±6 and 226±8 MeV at the center of the hydrogen target. These values have been corrected for beam contamination, energy loss in hydrogen, and increase in pion path length because of multiple Coulomb scattering in the copper absorber.

The composition of each incident beam was determined by means of pulse-height analysis of the radiation produced by the particles in a Čerenkov counter. The counter consisted of an aluminized Lucite tube filled with fluorochemical liquid, FC75,[16] having an index of refraction of 1.277 at 25°C. The tube, 2.75 in. in diameter and 10 and 24 in. in length for the 152- and 226-MeV measurements, respectively, was viewed by an RCA 7046 photomultiplier. The beam incident on the Čerenkov counter was defined by two small scintillation counters in coincidence. These detectors gated a 256-channel pulse-height analyzer to which was fed the output signal of the Čerenkov counter. Figure 1 is a typical spectrum obtained in analysis of the incident beam at 152 MeV. The three peaks, in the order of increasing pulse height, correspond to Čerenkov radiation produced by pions, muons, and electrons, respectively. The asymmetry of the peak at small pulse heights is presumably caused by pions whose path length has been shortened by nuclear interaction with the FC75. The spectrum was resolved into three separate maxima as indicated in the figure. Table I lists the beam compositions derived from the shape of the spectra obtained at 152, 185, and 226 MeV. The contamination decreases with increasing pion energy. The muon content of the beam determined in this way agrees with the results obtained through range measurements. The electron contamination, however, is larger than that deduced from range measurements, especially at 152 MeV.

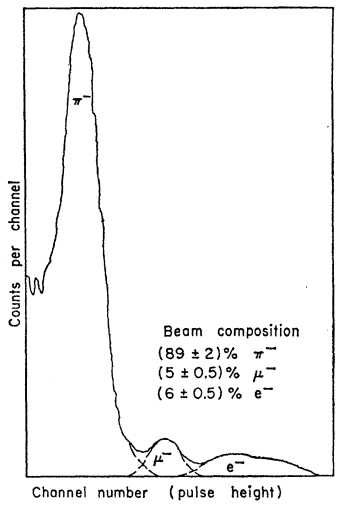

FIG. 1. Pulse-height spectrum obtained in analysis of the incident negative pion beam at 152 MeV.

TABLE I. Composition of negative pion beams.

Energy (MeV)	152±6	185±10	226±8
Pions (%)	89±2	91± 1	94±1
Muons (%)	5.0±0.5	5.5± 1.0	4.5±1.0
Electrons (%)	6.0±0.5	3.5± 1.0	1.5±1.0

Vertical and horizontal beam profiles were obtained by use of two small scintillation counters ($\frac{3}{8}\times\frac{3}{8}\times\frac{3}{8}$ in.) in coincidence with the monitor counters. The horizontal profile was folded into the circular cross section of the Mylar target to obtain the mean path length in hydrogen for the incident pions.

B. Scattering Geometry

1. Total Cross Section

A standard arrangement was employed in the transmission measurement of the total cross section. Counters 1, 2, and 3 in coincidence, designated as circuit C(123), monitored the incident beam. Each of these counters had dimensions of $1\frac{3}{4}\times1\frac{3}{4}\times\frac{1}{8}$ in. and $1\frac{1}{2}\times1\frac{1}{2}\times\frac{1}{8}$ in. for the 152- and 226-MeV experiments, respectively. A fourth counter, $6\frac{1}{2}\times6\frac{1}{2}\times\frac{1}{4}$ in., was placed behind the target at various distances from the target center.

To determine the effect of electronic drifts and to check the consistency of the data, it was desirable to make runs in which short, full, and empty target counts could be repeated alternately many times. For this purpose two identical styrofoam targets were constructed, one for use as full target and the other as empty target in the total cross-section measurement at 226 MeV. Because of the facility with which these targets could be interchanged, 144 short runs were made, each consisting of a full target count of about $1\frac{1}{2}$ min. duration followed by an empty target count. For this measurement, counter 4 was placed at a distance of 14 in. from the center of the target, subtending a half-angle of 13°.

[16] FC75, manufactured by Minnesota Mining and Manufacturing Company, St. Paul 6, Minnesota.

In addition to the styrofoam targets, the 152-MeV measurement utilized an aluminum target with Mylar windows that was designed to minimize background contribution. Counter 4 was placed at several distances from the target in order to check the consistency of scattering corrections.

2. *Differential Cross Section*

Figure 2 shows the scattering arrangement used in the measurement of the differential elastic cross section. Here again circuit C(123) monitored the incident meson beam. Counters 1, 2, 3, 4, and 5 in coincidence detected all charged particles scattered at angle θ_{lab}. Counter 5, with dimensions of $5\frac{1}{4}\times5\frac{1}{4}\times\frac{1}{4}$ in., defined the solid angle subtended by the detecting leg at the target. To prevent pions scattered by counter 3 from contributing background counts, counter $\bar{6}$ was placed in anticoincidence with counters 1, 2, 3, 4, and 5 in coincidence, forming circuit A(12345$\bar{6}$).

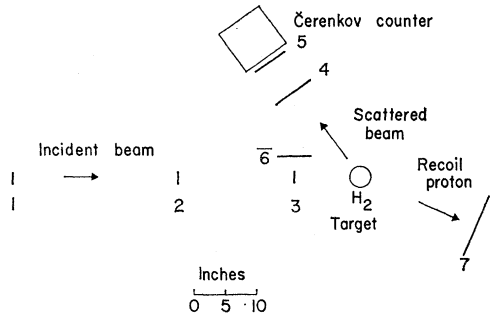

FIG. 2. Experimental arrangement for the measurement of the differential cross sections.

In order to differentiate between pions and electrons in the scattering telescope, a coincidence between the pions and the associated recoil protons was demanded in the angular range where the protons had sufficient energy to emerge from the target. This angular range varied from 155° to 127° and from 154° to 67° at 152 and 226 MeV, respectively. Counter 7, the recoil proton detector, had dimensions of $10\times10\times\frac{3}{8}$ in.; its position was determined from a graphical analysis utilizing the $\pi-\mathbf{P}$ scattering kinematics. The solid angle subtended by this counter at the target was made sufficiently large to permit the counting of all protons recoiling from detected pion scatterings. Thus the net counts obtained in a third circuit, B(123457$\bar{6}$), were due to scattered mesons only.

In the range of 113° to 30° and of 50° to 30° at 152 and 226 MeV, respectively, not all the recoil protons were sufficiently energetic to emerge from the target. In these angular regions, therefore, the spectra of pulse heights produced by the scattered particles in the Čerenkov counter placed behind counter 5 were utilized in distinguishing between π mesons and electrons. Such spectra were taken at all pion scattering angles. Figure 3, for example, is the spectrum obtained at 50° in the 226-MeV measurement.

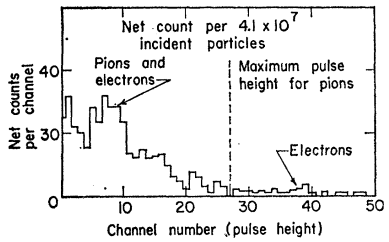

FIG. 3. Pulse-height spectrum obtained in analysis of the scattered beam at 50°. Pulse-height analysis of the incident beam, degraded to the energy of the pions scattered at 50°, yielded the indicated maximum pulse height produced by the pions.

At 155° scattered pions were below the threshold for producing Čerenkov radiation in FC75. Therefore, at this angle, the spectrum was produced by electrons only (after background subtraction). The simplifying assumption was made that this spectrum was the same as that produced by electrons at other angles as well. Figure 4 is the pulse-height spectrum obtained at 154° in the 226 MeV measurement. At the forward angles, the maximum pulse height produced by the mesons in the Čerenkov counter was determined by degrading the incident beam to the energies of pions scattered at each of these angles. Analysis of the spectra obtained from the scattered particles together with the spectra obtained from the degraded particles yielded the net number of electrons counted by the Čerenkov counter-analyzer system at the forward angles. These results were divided by λ, the efficiency of the counter analyzer in detecting electrons, to obtain the number of counts to be subtracted from $A(12345\bar{6})_{net}$ or $B(12345\bar{6})_{net}$ to give the net number of pions scattered at these forward angles.

A comparison of the net number of electrons counted by the Čerenkov counter-analyzer system with the net number of electrons counted by the π^--detecting leg at each angle in the range of 155° to 127° and of 154° to 67° at 152 and 226 MeV, respectively, yielded λ. At these angles the number of electrons counted by the π^--detecting leg is the difference between the net number of counts registered by circuit A(12345$\bar{6}$), detecting all scattered charged particles, and the net number of counts registered by circuit B(123457$\bar{6}$), detecting

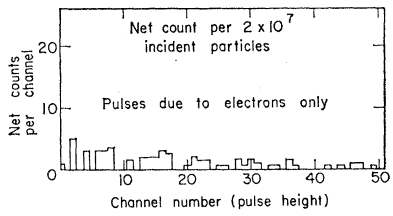

FIG. 4. Pulse-height spectrum obtained in analysis of the scattered beam at 154°. At this angle the pions were below the threshold for producing radiation in the Čerenkov detector. This spectrum was, therefore, produced by electrons only.

TABLE II. Electron contamination in scattered pion beams (% of total scattered particles).

152 MeV θ_{lab}	152 MeV Contamination	226 MeV θ_{lab}	226 MeV Contamination
30°	1.1±0.4	30°	11± 4
40°	1.9±2.3	40°	11± 4
55°	4.4±1.0	50°	14± 5
76°	9.6±2.1	67°[a]	29± 8
90°	14.9±3.2	80°[a]	26± 4
113°	20.8±4.2	95.5°[a]	11± 3
148°[a]	17.1±3.9	110°[a]	18±11
		125°[a]	4± 9
		140°[a]	11± 3
		154°[a]	14± 5

[a] At these angles, the detection of the recoil proton in coincidence with the scattered pion made it unnecessary to correct for the electrons present among the particles entering the pion telescope.

scattered mesons only. The average Čerenkov counter efficiency for detecting electrons was determined to be (65±19)% for the 152-MeV measurement and (66±13)% for the 226-MeV measurement.

Table II lists the fraction of electrons present among the scattered particles at all scattering angles in both the 152- and 226-MeV measurements. The table indicates that, to a first approximation, the fraction of electrons present among the scattered particles was constant at 226 MeV, while the contamination varied with angle for the 152-MeV measurement.

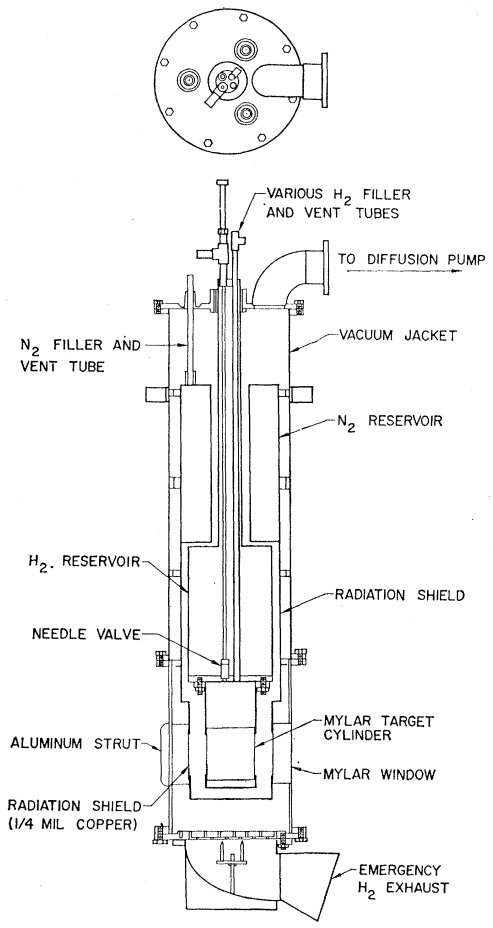

FIG. 5. Cutaway drawing of the liquid hydrogen target utilizing Mylar windows at beam level.

C. Liquid Hydrogen Targets

1. Aluminum—Mylar Target

Figure 5 is an assembly drawing of the aluminum target. The lower portion of the vacuum jacket had a window, 4 in. high, covering a full 360° except for two struts, $\frac{3}{4}$ in. wide, needed for structural support. Mylar sheets, glued to the aluminum housing with a thermosetting araldite,[17] provided the necessary windows for the incident beam. The Mylar, 3 mils thick, was aluminized to reduce heat transmission.

Liquid nitrogen and hydrogen reservoirs were suspended from the top plate of the vacuum jacket. The target cylinder, attached to the bottom plate of the hydrogen reservoir, consisted of Mylar in its central section and of stainless steel in its end sections. The cylindrical Mylar section, 3 mils thick and $3\frac{1}{4}$ in. in diameter, was glued to the stainless steel by means of a thermosetting araldite.[17] Hydrogen was fed into the target cylinder through a needle valve in the bottom plate of the hydrogen reservoir.

A Mylar diaphragm, 3 mils thick, was located at the base of the vacuum jacket. The design was such that the diaphragm would burst and the hydrogen would be exhausted should an abrupt rupture of the target cylinder occur. At pressures of the order of 5×10^{-5} mm Hg in the vacuum jacket, the rate of loss of hydrogen was about 50 cm³/h.

2. Styrofoam Target

The liquid hydrogen was contained in a rectangular parallelepiped which consisted of Mylar, 3 mils thick, stretched around a light tubular frame. The parallelepiped had the dimensions $3\frac{3}{4}\times3\frac{3}{4}\times10\frac{1}{2}$ in. and was placed inside a series of concentric styrofoam boxes. The design of the target was such that the cold effluent gases (hydrogen and nitrogen) were forced to flow downward over the walls of their respective containers. A total of 6 in. of styrofoam was in the pion beam. The loss rate of hydrogen was approximately 250 cm³/h.

D. Electronics

Figure 6 is a block diagram of the electronic arrangement used in the differential cross-section measurements. The scintillation counters utilized Pilot B plastic scintillants,[18] Lucite light pipes, and RCA 6810A photomultipliers. Pulses from the counters, after passing through variable timing delays, were appropriately

[17] Epibond 100A, manufactured by Furane Plastics, Inc., Los Angeles, California.

[18] Pilot B plastic scintillant, produced by Pilot Chemicals Inc., Watertown 72, Massachusetts.

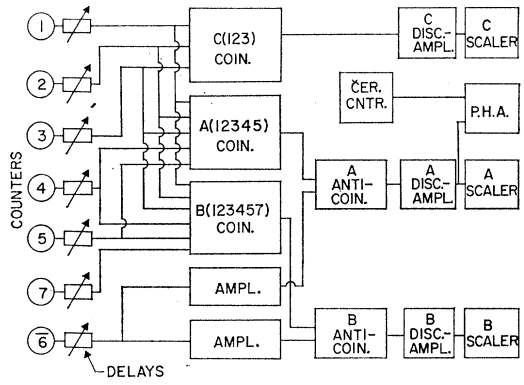

FIG. 6. Block diagram of the electronics used in the measurement of the differential cross sections.

combined in three separate coincidence circuits; C(123) monitored the incident beam; A(12345$\bar{6}$) registered the number of charged particles in the scattering telescope; B(123457$\bar{6}$) recorded scattered pions. The coincidence circuits were modified Garwin-type circuits of Berkeley design[19] with resolving times of the order of 10 nsec. The output signal of the Čerenkov counter placed behind counter 5 was fed into a 256-channel pulse-height analyzer, gated by circuit A(12345$\bar{6}$).

III. DATA REDUCTION AND ANALYSIS

A. Total Cross Section

The total cross section σ was determined from the transmission with full and empty target according to the equation:

$$\left[\frac{A(1234)}{C(123)}\right]_{\text{Full target}}=\left[\frac{A(1234)}{C(123)}\right]_{\text{Empty target}}e^{-N\sigma}.$$

N, the net number of protons per unit area, was equal to 4.04×10^{23} cm^{-2} and 3.16×10^{23} cm^{-2} in the 226- and 152-MeV measurements, respectively.

The uncorrected cross section obtained at 226 MeV is 47.4±1.2 mb. The error assigned is 3 times the root mean square deviation of the 144 measured cross sections from their mean value. The factor 3 was arbitrarily chosen to give a more realistic appraisal of the actual uncertainty in the measurement. The large uncertainty is caused by variations of approximately 1% in transmissions with full and empty target. These variations may have been produced by random fluctuations in discriminator levels in the coincidence circuits. That the fluctuations were random is indicated by the graph of Fig. 7. The fraction of measured cross sections having magnitudes less than a value Σ is plotted as a function of Σ. The ordinate, or probability, scale is arranged in such a manner that a Gaussian distribution results in a linear plot.

[19] Lawrence Radiation Laboratory Counting Handbook, UCRL 3307 Rev., File No. CC3-6, 1956 (unpublished).

At 152 MeV, uncorrected cross sections of 53.7±1.3 mb and 55.4±1.1 mb were obtained with counter 4 subtending half-angles of 16° and 13°, respectively. For each half-angle, four pairs of full and empty transmissions were measured with the aluminum-Mylar target in place. Approximately 10^6 counts were recorded for each transmission. In addition, with the styrofoam target in place, 100 pairs of full and empty target transmissions were measured. An uncorrected cross section of 54.4±0.8 mb was obtained, the uncertainty being the expected standard deviation.

In order to obtain the "true" total cross section for π^- mesons scattered by protons, corrections[20] for the following effects were applied to the "raw" cross sections:

(1) μ mesons and electrons that contaminated the incident beam were transmitted through the target with the result that the uncorrected transmission corresponded to a smaller π^-p cross section than the actual one.

(2) Forward-scattered mesons or recoil protons associated with backscattered mesons were detected by counter 4, thereby reducing the measured cross section. The correction for this effect was calculated using the corrected measured elastic π^-p angular distribution which was numerically integrated over the solid angle subtended by the transmission counter at the center of the target.

(3) In the scattering of pions by protons, the Coulomb amplitude interferes with the nuclear amplitude. To a good approximation, the complete scattering amplitude is the sum of the nuclear and Coulomb amplitudes.[21–23] The contribution of Coulomb scattering to the measured transmission was therefore calculated with the help of approximate scattering phase shifts,[6,7]

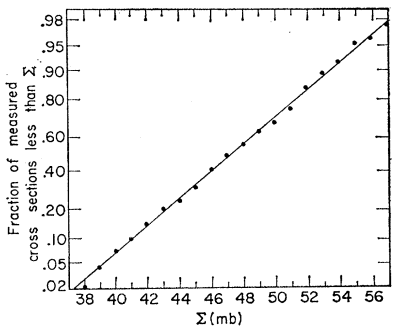

FIG. 7. Fraction of the measured total cross sections at 226 MeV having a magnitude less than a value Σ plotted as a function of Σ. The ordinate, or probability, scale is arranged in such a manner that a Gaussian distribution results in a linear plot.

[20] For detailed derivations of the corrections, see W. P. Kovacik, Carnegie Institute of Technology Report NYO-2242, 1960 (unpublished); S. Kellman, Carnegie Institute of Technology Report NYO-9281, 1960 (unpublished).

[21] L. van Hove, Phys. Rev. **88**, 1358 (1952).

[22] J. Ashkin and L. Smith, Carnegie Institute of Technology Technical Report No. 1, 1953 (unpublished).

[23] F. T. Solmitz, Phys. Rev. **94**, 1799 (1954).

TABLE III. Corrections (in mb) to total cross-section data.

Energy (MeV)	Target	Uncorrected cross section	1[a]	2	3	4	Corrected cross section (mb)
152	Mylar	53.7±1.3[b]	6.6±1.2	4.9±0.2	−0.8	−0.6	63.8±1.9
152	Mylar	55.4±1.1	6.9±1.2	3.1±0.2	−1.0	−0.6	63.7±1.7
152	Styrofoam	54.4±0.8	8.1±1.3	3.1±0.2	−1.0	−0.6	64.0±1.6
226	Styrofoam	47.4±1.2	3.0±0.5	3.0±0.2	+0.1	−0.6	52.9±1.4

[a] Corrections are identified in Sec. III A.
[b] Measurement made with transmission counter subtending half-angle of 16° at center of target. All other measurements made with 13° half-angle.

taking the difference between the differential cross sections with and without the inclusion of the Coulomb term. The correction to the total cross section was obtained by integrating this difference over the solid angle subtended by the transmission counter at the center of the target.

(4) The measured transmission was reduced by counts due to the radiative capture process, $\pi^-+p\rightarrow n+\gamma$. The magnitude of the correction was obtained by application of the principle of detailed balancing to the inverse reaction, $\gamma+n\rightarrow\pi^-+p$.

The magnitudes of the corrections applied to the transmission data are listed in Table III. The corrected total cross sections obtained at 152 and 226 MeV are 63.7±2.0 and 52.9±1.4 mb, respectively.

B. Differential Cross Section

The differential cross section was determined from the equation:

$$d\sigma(\theta_{\rm lab})/d\Omega=n(\theta_{\rm lab})/N\Omega_0,$$

where $n(\theta_{\rm lab})$ is the number of particles scattered at angle $\theta_{\rm lab}$ per incident particle; Ω_0 is the solid angle subtended by counter 5 at the center of the target, and N is the net number of scattering centers per unit area. The value of N, reduced by 1.8% to account for the cold hydrogen gas that remained in the target during the empty target measurement, was 3.16×10^{23} cm^{-2} and 3.28×10^{23} cm^{-2} for the 152- and 226-MeV experiments, respectively. The increase in the value of N at 226 MeV is due to the use of smaller monitor counters limiting the incident beam to the more central region of the cylindrical Mylar target.

1. Corrections

The first five corrections[20] applied to the uncorrected differential cross sections are angle independent and the remaining six are angle dependent. The statistical accuracy of the experiments was approximately 3% and corrections of the order of 0.5% or greater were considered. Listed in Tables IV and V are correction factors for the following effects:

(a) The incident beam was composed of π mesons, μ mesons, and electrons.

(b) Since the incident pion flux was attenuated as the beam traversed the liquid hydrogen, the beam intensity at the center of the target should have been used as the effective incident flux.

(c) Counters 3 and 4 and the walls of the target assembly could scatter and absorb mesons.

(d) Accidental coincidences in the monitor tended to decrease the measured cross section. An upper limit to the number of accidental counts in the monitoring leg was obtained when counters 1, 2, and 3, in line, were placed in the incident beam. The correction, neglected at 226 MeV, resulted in an increase of (0.6±0.5)% in the differential cross section at 152 MeV.

(e) Dead-time losses of the coincidence circuits tended to increase the measured cross section. The counting rates of circuits C(123), A(123), and A(12345)

TABLE IV. Correction factors[a] for differential cross-section data at 152 MeV.

$\theta_{\rm lab}$	(f)	(g)	(h)	(i)	(j)	Net correction factor[b]×(1.000±0.024)$^{-1}$
30°	1.010	1.117±0.015	1.000	1.008±0.010	0.905	1.170±0.020
40°	1.010	1.092±0.022	0.999	1.008±0.010	0.939	1.187±0.029
55°	1.012	1.025±0.027	0.993	1.006±0.010	0.962	1.144±0.032
76°	1.013		0.998	1.004±0.010	0.990	1.152±0.013
90°	1.013		0.989	1.003±0.010	1.008	1.162±0.013
113°	1.012		0.998	1.001±0.010	1.015	1.177±0.013
127°	1.012		1.000	1.000±0.010	1.013	1.167±0.013
134°	1.011		1.001	1.000±0.010	1.013	1.167±0.013
141°	1.011		1.001	0.999±0.010	1.012	1.165±0.013
148°	1.010		1.001	0.999±0.010	1.011	1.163±0.013
155°	1.010		1.002	0.999±0.010	1.011	1.164±0.013

[a] Corrections are identified in Sec. III B. Angle-independent correction factors are (a) 1.124±0.025; (b) 1.010; (c) 1.013; (d) 1.006±0.005; and (e) 0.986±0.010. Net angle-independent correction factor: 1.137±0.027.
[b] The angle-independent uncertainty in the differential cross section is ±2.4%.

TABLE V. Correction factors[a] for differential cross-section data at 226 MeV.

θ_{lab}	(f)	(g)	(h)	(i)	(j)	Net correction factor[b] $\times(1.000\pm0.012)^{-1}$
30°	1.011	1.220±0.012	1.000±0.005	1.004±0.010	1.030	1.389±0.021
40°	1.012	1.163±0.012	1.000±0.005	1.005±0.010	1.012	1.303±0.200
50°	1.013	1.130±0.011	0.999±0.005	1.006±0.010	1.004	1.258±0.019
67°	1.014	1.036±0.010	0.993±0.005	1.008±0.010	0.991	1.135±0.017
80°	1.014		0.986±0.005	1.009±0.010	0.984	1.081±0.012
95.5°	1.014		0.997±0.005	1.012±0.010	0.981	1.093±0.012
110°	1.014		0.999±0.005	1.014±0.010	0.982	1.098±0.012
125°	1.013		1.000±0.005	0.979±0.010	0.988	1.067±0.012
140°	1.012		1.000±0.005	0.992±0.010	0.990	1.082±0.012
154°	1.011		1.000±0.005	0.998±0.010	0.991	1.089±0.012

[a] Corrections are identified in Sec. III B. Angle-independent correction factors are: (a) 1.064±0.011; (b) 1.009; (c) 1.014; (d) 1.000; (e) 1.000. Net angle-independent correction factor: 1.089±0.013.
[b] The angle-independent uncertainty in the differential cross section is 1.2%.

were measured as a function of incident beam rate, monitored by an auxiliary counter telescope which sampled only a small portion of the incident beam. Dead-time losses were negligible in most cases. Circuit C(123), however, had a dead-time loss of (1.4±1.0)% at the counting rate of 3500 mesons per sec at 152 MeV.

The net angle independent correction factor was 1.137±0.027 and 1.089±0.013 at 152 and 226 MeV, respectively.

TABLE VI. Differential cross sections at 152 MeV.

$\theta_{c.m.}$	$d\sigma/d\Omega\times(1.000\pm0.024)^{-1}$ in mb/sr
38.0°	2.56±0.07
50.0°	2.05±0.09
67.5°	1.43±0.05
90.5°	0.98±0.05
104.5°	0.98±0.05
126.0°	1.33±0.10
138.0°	1.63±0.04
144.0°	1.81±0.05
149.5°	1.89±0.04
155.0°	2.08±0.06
160.5°	2.17±0.09

TABLE VII. Differential cross sections at 226 MeV.

$\theta_{c.m.}$	$d\sigma/d\Omega\times(1.000\pm0.012)^{-1}$ in mb/sr
39.7°	2.12±0.14
52.3°	1.72±0.11
64.4°	1.33±0.10
83.7°	0.75±0.03
97.3°	0.63±0.03
112.4°	0.82±0.02
125.5°	1.12±0.05
138.1°	1.63±0.06
150.2°	1.92±0.06
160.9°	2.22±0.08

(f) Due to the finite size of the target cylinder and the planar nature of the defining counter, a correction to the solid angle Ω_0 was necessary.

(g) At the forward angles, Lucite and carbon absorbers were placed behind counter 4 to prevent recoil protons associated with backscattered mesons from being counted by the π^--detecting leg. The resulting attenuation of the pions was measured by placing the detecting system in an incident pion beam whose energy was degraded to correspond to the energy of the pions scattered at any given angle.

(h) Due to the finite angular resolution (about ±10°) of defining counter 5, the differential cross section measured at a given angle θ was a cross section averaged over the range of angles at which scatterings were detected.

(i) Double elastic scattering of mesons and protons in hydrogen and the walls of the target assembly could have altered the angular distribution of the pions.

(j) As discussed in the preceding section, the Coulomb amplitude interferes with the nuclear amplitude in $\pi^- - p$ scattering.

The question of whether any scattered mesons were not detected due to π-μ decay was investigated by Feiner.[24] He found that although it was possible for such decays to "scatter out" a pion, the compensating mechanism of "scattering in" made the net effect negligible.

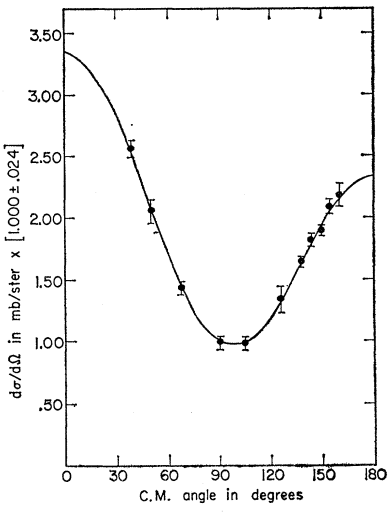

FIG. 8. Differential elastic cross section measured at 152 MeV. The solid curve is the least-squares fit to the data.

[24] F. Feiner, thesis, Carnegie Institute of Technology, 1955 (unpublished.)

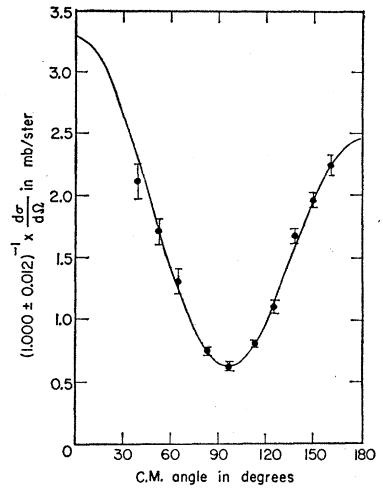

FIG. 9. Differential elastic cross section measured at 226 MeV. The solid curve is the least-squares fit to the data.

Corrections for the following effects were also found to be negligible: detection of charge exchange scattering, multiple scattering in the hydrogen or counter 4, and scattering of the electrons present in the incident beam by the hydrogen.

The final corrected differential cross sections are tabulated in Tables VI and VII, and plotted in Figures 8 and 9.

2. *Least-Squares Analysis*

The assumption was made in performing a least-squares analysis of the nuclear differential cross-section data that only S and P waves contribute appreciably to the scattering. As a consequence of this assumption, the differential cross section in the center-of-mass system may be expressed as

$$d\sigma(\theta)/d\Omega = (1\pm d)(a+b\cos\theta+c\cos^2\theta).$$

The values of the coefficients obtained at each energy are listed in Tables VIII and IX.

An indication of the quality of the fit is given by the value of

$$M=\sum_i \epsilon_i^2,$$

where ϵ_i is the deviation of the ith experimental point from the fitted curve, expressed in units of the uncertainty in that point. Values of M of 1.6 and 4.9 were obtained at 152 and 226 MeV respectively, while the expected values were 8 and 7.[25] A small value of M would result if the assigned errors were too large. It is felt, however, that the errors assigned at 152 MeV are not excessively pessimistic. The good fit to the data is therefore real. These results, then, support the hypothesis that D waves are not appreciable in the 150- and 220-MeV regions.

TABLE VIII. Summary of experimental results in the 150-MeV region.

	Ashkin[b]	Kruse[c]	This experiment
Energy (MeV)	150 ±7	150	152 ±6
σ_{el}^-(mb)	20.0	18.9	20.1 ±0.5
σ_{total} (mb)	55.3 ±1.6	60.0 ±2.3	63.7 ±2.0
a[a] (mb/sr)	0.97±0.03	0.84	0.98±0.03
b (mb/sr)	0.44±0.05	0.45	0.51±0.04
c (mb/sr)	1.87±0.10	1.99	1.86±0.07
$\sigma_{el}^-/\sigma_{total}$	0.36	0.32	0.32±0.01

[a] The π^--elastic differential cross section is expressed as $d\sigma/d\Omega=(1\pm d)\times(a+b\cos\theta_{c.m.}+c\cos^2\theta_{c.m.})$.
[b] See reference 6.
[c] See reference 13.

IV. CONCLUSIONS AND DISCUSSION

Tables VIII and IX show the results of recent experiments on the scattering of negative pions by protons in the 150- and 220-MeV regions. The results of the Chicago and the present total cross-section measurements at 152 MeV may be in better agreement than is indicated. The contamination of the incident beam in the Chicago experiment was obtained through range measurements. In the present experiment, however, determination of the contamination by range measurements and by pulse-height analysis of the radiation produced by the particles in a Čerenkov counter indicated that the electron contamination was 5% greater than the value estimated from range measurements. If, then, the electron contamination of the incident beam in the Chicago experiment were increased, the resulting increase in cross section would bring the two results into better agreement.

The total cross section obtained by the present authors at 152 MeV does not agree with the previous value obtained by Ashkin *et al.*,[6] even after a 3% correction is made for additional incident beam contamination. In contrast, the total cross-section results in the 220 MeV region are in good agreement.

The discrepancies between the differential cross sections measured by the present authors and those obtained previously by Ashkin *et al*[6,7] may be explained by the undetected presence of electrons in the scattered pion beam during the earlier measurements. The electron contamination observed in the present experiment at 152 MeV varied from approximately 20% at the backward angles to 1% at the forward angles. The decrease in the cross section at the backward angles produced by the contamination correction is expressed by an increase in the value of coefficient b. Comparing the present results at 152 MeV with the Chicago data as in Table VIII, one finds that the values of the coefficients b and c agree within the errors while the Chicago value of a is lower than that obtained in the present experiment.

As can be seen from Fig. 10, the differential cross sections measured previously at 220 MeV agree with the $d\sigma/d\Omega$ obtained by use of the present data of circuit A(12345$\bar{6}$) which detected all charged particles. All the corrections discussed above have been applied

[25] H. Cramer, *Mathematical Methods of Statistics* (Princeton University Press, Princeton, New Jersey, 1946).

TABLE IX. Summary of experimental results in the 220-MeV region.

	Ashkin[b]	Deahl[c]	This experiment	Goodwin[d], Caris[e]	Zinov[f]
Energy (MeV)	220 ±7	224 ±10	226 ±8	230 ±8	240 ±7
σ_{el}^- (mb)	19.5 ±0.6	16.0 ± 0.8	17.4 ±0.3	20.8 ±0.4	16.1 ±0.6
σ_{total} (mb)	53.2 ±1.5	50.5 ±2.1	52.9 ±1.4	58 ±9	48.3 ±3.3
a[a] (mb/sr)	0.86±0.06	0.70±0.04	0.66±0.02	0.95±0.04	0.81±0.08
b (mb/sr)	0.30±0.08	0.33±0.07	0.41±0.05	0.55±0.06	0.23±0.09
c (mb/sr)	2.07±0.18	1.69±0.13	2.16±0.08	2.10±0.09	1.41±0.18
$\sigma_{el}^-/\sigma_{total}$	0.37±0.02	0.32±0.02	0.33±0.01	0.36±0.06	0.33±0.03

[a] The π^--elastic differential cross section is expressed as $d\sigma/d\Omega = (1 \pm d)(a + b\cos\theta_{c.m.} + c\cos^2\theta_{c.m.})$.
[b] See reference 7.
[c] See reference 15.
[d] See reference 26.
[e] J. C. Caris, L. K. Goodwin, R. W. Kenney, V. Perez-Mendez, and W. A. Perkins, III, Phys. Rev. 122, 262 (1961).
[f] V. G. Zinov and S. M. Korenchenko, Soviet Phys.—JETP 9, 429 (1959).

to the A circuit data except for the elimination of the electrons in the scattered beam. Indeed, if σ_{el}^- as determined by Ashkin *et al*[7] is decreased by the 15% electron contamination of the scattered beam as found in the present experiment at 226 MeV, good agreement between the values of the total π^- elastic cross section is achieved. This same feature may explain the discrepancy between the present results and those of the counter experiment of Goodwin.[26] Most of the present findings at 226 MeV are in accord with those of the bubble chamber experiment of Deahl[15]; σ_{el}^-, a and b agree fairly well while there appears to be a considerable discrepancy in the c coefficient. The results of the experiments in the 150- and 220-MeV regions indicate that the ratio, $\sigma_{el}^-/\sigma_{total}$, is approximately $\frac{1}{3}$. This is the result expected if, under the assumption of charge independence of the pion-nucleon interaction, the contribution from the isotopic spin $\frac{1}{2}$ state is small compared to that from the $\frac{3}{2}$ state.

The phase shifts obtained by Ashkin, Deahl, and the present authors at 220 MeV are listed in Table X.

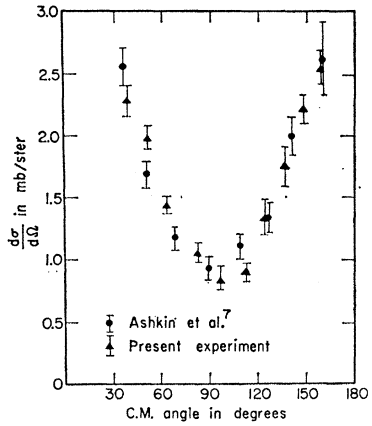

FIG. 10. The differential elastic cross section measured at 220 MeV by Ashkin *et al.* (reference 7) and the present result obtained at 226 MeV using circuit A(123456) which detected all charged particles in the scattered beam. All the corrections discussed in the text have been applied to the A circuit data except for the elimination of the electrons in the scattered beam.

[26] L. K. Goodwin, R. W. Kenney, and V. Perez-Mendez, Phys. Rev. 122, 655 (1961).

The phase shifts agree quite well, especially in the most important feature—the magnitude of α_{33}.

Finally, the present experimental data may be used to calculate the value of D_-^b, the real part of the forward-scattering amplitude in the c.m. system, for comparison with the theoretical results obtained by use of dispersion relations. The calculations result in $D_-^b = 0.190^{+0.021}_{-0.027}$ and $-0.129^{+0.061}_{-.0400}$ at 152 and 226 MeV, re-

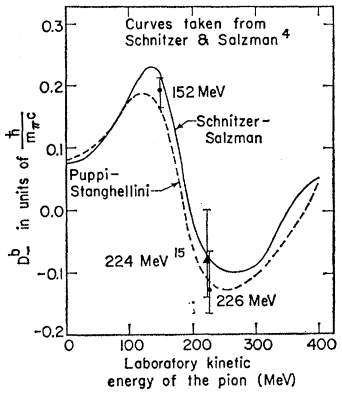

FIG. 11. The real part of the forward-scattering amplitude in the c.m. system, D_-^b, in units of $\hbar/m_\pi c$ plotted as a function of laboratory kinetic energy of the pions. As indicated, the dashed and solid curves are the results obtained by Puppi and Stanghellini (reference 3) and by Schnitzer and Salzman (reference 4), respectively, with dispersion relations using a coupling constant of $f^2=0.08$. The experimental points at 152 MeV and 226 MeV represent the data of the present experiments. The point at 224 MeV is the work of Deahl (reference 15).

TABLE X. Phase shifts at 225 MeV.

	Ashkin[a]	Deahl[b]	This experiment[c]
α_1	15.0°	14.8±3.5°	12.6°
α_3	−14.5°	−15.5±3.5°	−17.5°
α_{11}	7.0°	5.9±4.5°	4.0°
α_{13}	− 5.0°	0.0±2.0°	− 2.4°
α_{31}	− 5.0°	− 2.1±5.5°	− 7.3°
α_{33}	112.0°	112.3±3.0°	111.0°

[a] See reference 7.
[b] See reference 15.
[c] These phase shifts were determined with a program written for the IBM 650 computer by Deahl.

spectively. The uncertainty assigned takes account of correlated errors.

Figure 11 is a plot of D_-^b versus pion energy, as obtained by Schnitzer and Salzman[4] and by Puppi and Stanghellini.[3] With the uncertainty assigned, the values of D_-^b obtained in the present experiments agree with the theoretical curves of Schnitzer and Salzman, and Puppi and Stanghellini and the considerations of Noyes and Edwards.[14] It, therefore, appears that the experimental results for the absolute value of the real part of the forward-scattering amplitude are now in agreement with the theoretical values obtained by use of dispersion relations.

ACKNOWLEDGMENTS

We wish to thank Professor Julius Ashkin for his aid and guidance in the design, performance, and analysis of these experiments. The assistance of William Chu in building and maintaining the equipment and in taking the data was also greatly appreciated.

PHYSICAL REVIEW VOLUME 129, NUMBER 1 1 JANUARY 1963

Recoil Study of the Reaction $Al^{27}(p,3pn)Na^{24}$*

A. M. POSKANZER, J. B. CUMMING, AND R. WOLFGANG†
Chemistry Department, Brookhaven National Laboratory, Upton, New York
(Received 15 August 1962)

In order to study the mechanism of a simple spallation reaction induced by GeV-energy protons, measurements were made of the momentum properties of Na^{24} nuclei produced from an aluminum target. Data were obtained on: (1) the fraction of Na^{24} nuclei recoiling out of targets thick with respect to the range of the recoils (the targets were oriented both perpendicular and parallel to the proton beam); (2) the distribution of Na^{24} ranges from a thin target measured with plastic catchers subtending an angle of 2π; (3) the angular distribution of the Na^{24} recoils with respect to the beam. Results of Monte Carlo knock-on cascade and evaporation calculations for 0.36- and 1.8-GeV bombarding energies are compared with the data in the laboratory system. The calculations predict sharper sideways peaking in the angular distributions, and more momentum deposition at the higher bombarding energy, than are observed. The experimental data are also reduced to a set of velocity vectors which is then interpreted in terms of a simple, constant-deposition-energy mechanism in which the incident proton makes only one quasi-elastic collision with a single nucleon which does not escape from the nucleus. This treatment accounts for most of the data but also predicts a much larger sideways peaking in the angular distribution than is observed.

INTRODUCTION

THE basic model of high-energy nuclear reactions,[1] that of a nucleonic cascade followed by nuclear evaporation, has been used in various degrees of refinement to calculate cross sections of spallation reactions. However, the recoil momentum of the residual nucleus should be more sensitive to the mechanism of formation than measurements of only the formation cross section. For this reason the present recoil measurements were undertaken and compared with the predictions of various forms of the basic high-energy reaction model.

The recoil properties of Na^{24} produced by bombardment of aluminum with protons had been studied by Hintz[2] up to 90 MeV, by Fung and Perlman[3] up to 340 MeV, by Volkova and Denisov[4] and Crespo[5] at 660 MeV, and by Wolfgang and Friedlander[6] up to 2.2 GeV. All of these experiments were measurements of the fraction of Na^{24} recoiling out of an aluminum target thick compared to the range of the recoils. The present experimental work extends these measurements and presents more detailed experiments on thin targets to obtain information on the angular distribution and differential range of the recoils.

The ideal radiochemical recoil experiment, which would give the most information about the momentum of the recoil, would be a differential range measurement at many different angles to the beam. However, because of the limitations of beam intensity and time, less detailed experiments have been done. The thick-target experiments, the easiest to perform and the only kind extensively studied in the past, measure average momenta projected along a particular axis. The more detailed 2π differential-range curves measure the distribution in magnitude of the momenta averaged over angle. The angular distribution measurements, integrate over all momenta at a particular angle.

Two approaches have been used in the interpretation of the recoil data. The first is based on Monte Carlo knock-on cascade calculations[7] which kept track of the

* Research performed under the auspices of the U. S. Atomic Energy Commission.
† Present address: Yale University, New Haven, Connecticut.
[1] J. M. Miller and J. Hudis, Ann. Rev. Nucl. Sci. **9**, 159 (1959).
[2] N. M. Hintz, Phys. Rev. **86**, 1042 (1952).
[3] S. C. Fung and I. Perlman, Phys. Rev. **87**, 622 (1952).
[4] V. Volkova and F. P. Denisov, J. Exptl. Theoret. Phys. (U.S.S.R.) **35**, 538 (1958).
[5] V. P. Crespo, University of California Radiation Laboratory Report UCRL 9683, 1961 (unpublished).
[6] R. Wolfgang and G. Friedlander, Phys. Rev. **94**, 775 (1954).
[7] N. Metropolis, R. Bivins, M. Storm, A. Turkevich, J. M. Miller, and G. Friedlander, Phys. Rev. **110**, 185 (1958); N.